EUMETSAT Satellite Application Facility on Climate Monitoring
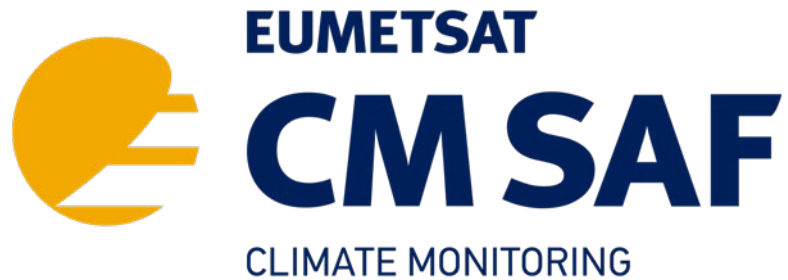

Algorithm Theoretical Basis Document

Land Surface Temperature (LST)

Edition 2

Document Signature Table

	Name	Function	Signature	Date
Author	Anke Duguay-Tetzlaff Virgílio A. Bento Reto Stöckli	CM SAF Scientist LSA SAF Visiting Scientist CM SAF Scientist	*Anke Duguay-Tetzlaff*	
Editor	Marc Schröder	CM SAF Science Coordinator		
Approval	CM SAF Steering Group			
Release	Rainer Hollmann	CM SAF Project Manager		

Distribution List

Internal Distribution	
Name	No. Copies
DWD Archive	1
CM SAF Team	1

External Distribution		
Company	Name	No. Copies
PUBLIC		1

Document Change Record

Issue/ Revision	Date	DCN No.	Changed Pages/Paragraphs
1.0	30/07/2015	SAF/CM/MeteoSwiss/ATBD/MET/LST/1	First official version.
1.1	27/11/2015	SAF/CM/MeteoSwiss/ATBD/MET/LST/1	Included suggestions from reviewers during PCR 2.8/2.9.
2.0	26/05/2020	SAF/CM/MeteoSwiss/ATBD/MET/LST/2	Included updates on the Meteosat calibration and emissivity data.
2.1	15/01/2021	SAF/CM/MeteoSwiss/ATBD/MET/LST/2	Included updates from PCR3.9

Applicable documents

Reference	Title	Code
AD 1	CM SAF Product Requirements Document	SAF/CM/DWD/PRD/4.1

Reference documents

Reference	Title	Code
RD 1	Product User Manual LST product edition 1	SAF/CM/DWD/PUM/LST/1
RD 2	Validation Report LST product edition 1	SAF/CM/DWD/VAL/LST/1
RD 3	Algorithm Theoretical Basis Document Meteosat Cloud Fractional Cover (CFC) Edition 1	SAF/CM/MeteoSwiss/ATBD/MET/CFC/2
RD 4	Algorithm Theoretical Basis Document Land Surface Temperature (LST) 1.2	SAF/LAND/IM/ATBD/LST/1.2

Table of Contents

List of Tables

List of Figures

1   The EUMETSAT SAF on Climate Monitoring (CM SAF)

The importance of climate monitoring with satellites was recognized in 2000 by EUMETSAT Member States when they amended the EUMETSAT Convention to affirm that the EUMETSAT mandate is also to "contribute to the operational monitoring of the climate and the detection of global climatic changes". Following this, EUMETSAT established within its Satellite Application Facility (SAF) network a dedicated centre, the SAF on Climate Monitoring (CM SAF, http://www.CM SAF.eu).

The consortium of CM SAF currently comprises the Deutscher Wetterdienst (DWD) as host institute, and the partners from the Royal Meteorological Institute of Belgium (RMIB), the Finnish Meteorological Institute (FMI), the Royal Meteorological Institute of the Netherlands (KNMI), the Swedish Meteorological and Hydrological Institute (SMHI), the Meteorological Service of Switzerland (MeteoSwiss), and the Meteorological Service of the United Kingdom (UK MetOffice). Since the beginning in 1999, the EUMETSAT Satellite Application Facility on Climate Monitoring (CM SAF) has developed and will continue to develop capabilities for a sustained generation and provision of Thematic Climate Data Records (TCDR's) derived from operational meteorological satellites.

In particular the generation of long-term products is pursued. The ultimate aim is to make the resulting products suitable for the analysis of climate variability and potentially the detection of climate trends. CM SAF works in close collaboration with the EUMETSAT Central Facility and liaises with other satellite operators to advance the availability, quality and usability of Fundamental Climate Data Records (FCDR's) as defined by the Global Climate Observing System (GCOS). As a major task the CM SAF utilizes FTCDR's to produce records of Essential Climate Variables (ECVs) as defined by GCOS. Thematically, the focus of CM SAF is on ECVs associated with the global energy and water cycle.

Another essential task of CM SAF is to produce products that can serve applications related to the new Global Framework of Climate Services initiated by the WMO World Climate Conference-3 in 2009. CM SAF is supporting climate services at national meteorological and hydrological services (NMHSs) with long-term data records but also with products produced close to real time that can be used to prepare monthly/annual updates of the state of the climate. Both types of products together allow for a consistent description of mean values, anomalies, variability and potential trends for the chosen ECVs. CM SAF ECV products also serve the improvement of climate models both at global and regional scale.

As an essential partner in the related international frameworks, in particular WMO SCOPE-CM (Sustained COordinated Processing of Environmental satellite data for Climate Monitoring), the CM SAF - together with the EUMETSAT Central Facility, assumes the role as main implementer of EUMETSAT's commitments in support to global climate monitoring. This is achieved through:

- Application of highest standards and guidelines as lined out by GCOS for the satellite data processing,
- Processing of satellite data within a true international collaboration benefiting from developments at international level and pollinating the partnership with own ideas and standards,
- Intensive validation and improvement of the CM SAF climate data records,
- Taking a major role in product assessments performed by research organisations such as WCRP (World Climate Research Program). This role provides the CM SAF with deep contacts to research organizations that form a substantial user group for the CM SAF TCDR's,
- Maintaining and providing an operational and sustained infrastructure that can serve the community within the transition of mature TCDR products from the research community into operational environments.

A catalogue of all available CM SAF products is accessible via the CM SAF webpage, www.CM SAF.eu. Here, detailed information about product ordering, add-on tools, sample programs and documentation is provided.

2   Introduction

This Algorithm Theoretical Basis Document (ATBD) explains the physical and mathematical background for an algorithm to derive Land Surface Temperature (LST) from Meteosat First Generation (MFG) and Meteosat Second Generation (MSG) satellites. Important features of the CM SAF LST TCDR are:

- Long-term climate data record for LST dating back until 1991. Those multi-decadal characteristics make the data very well suited for climate analysis.

- The high temporal (≤ 30 min) and high spatial resolution (≤ 5 km) of the MVIRI and SEVIRI instrument allow a sufficient temporal and spatial sampling of LST. Hence, the data can provide accurate estimates of monthly diurnal cycle information for a physical variable which varies strongly in time and space. The presented TCDRs are complementary to existing TCDRs from polar orbiting satellites such as ISCCP.

- The SEVIRI field of view covers a fairly large domain of the globe. For the regions covered (e.g. Europe, Africa, Atlantic Ocean) this allows the monitoring of climate variability.

The CM SAF LST algorithm is part of the GeoSatClim processing package **[RD 2]**, developed at the Swiss Federal Office of Meteorology and Climatology MeteoSwiss (http://www.meteoswiss.admin.ch) within CM SAF's second Continuous Development and Operations Phase (CDOP-2). Beside the LST algorithm, the GeoSatClim processing package **[RD 2]** also includes algorithms for the generation of cloud mask, cloud amount, cloud fractional cover and tropospheric humidity across Meteosat satellite generations.

The presented LST algorithm was established in the framework of an EUMETSAT Land Surface Analysis Satellite Applications Facility (LSA SAF) – CM SAF Federated Activity. The LSA SAF provides operational LST products for Meteosat since 2005 (lsa-saf.eumetsat.int). The intention of this Federated Activity was to develop an LST algorithm suitable to generate a 30 year+ long Meteosat LST TCDR, starting in the early 1980s. The LSA SAF retrieves LST from MSG using the established Generalized Split-Window algorithm **[RD 4]**. In a joint effort the LSA SAF and CM SAF team have developed a single-channel LST algorithm, suitable to generate LST's across Meteosat satellite generations. A consistent, single-channel approach maximizes long-term and inter-satellite consistency (Scarino et al. 2013). The single-channel algorithm, outlined in this document, is consistent with the current LSA SAF algorithm **[RD 4]** in terms of error characterization and model validation.

The CM SAF LST TCDR is derived from geostationary Meteosat satellite data. Existing LST TCDR's are based on polar orbiters, which cannot capture diurnal LST variations. Geostationary satellites, with a high temporal resolution, provide an unique opportunity to estimate the diurnal LST cycle (Sun et al. 2006) which is an important climate change indicator (Karl et al. 1993). The Meteosat system has continuously been acquiring data in the thermal infrared for well over 30 years over Africa and Europe. The MFG satellites carried the Meteosat Visible and InfraRed Imager (MVIRI) instrument. The MVIRI sensor provides 3 spectral measurements in the visible, in the water vapour and in the infrared domain. Starting in 2002, the Spinning Enhanced Visible and InfraRed Imager (SEVIRI) instrument is operated on EUMETSAT's MSG satellites. The SEVIRI instrument performs 12 spectral measurements, including two measurements in the thermal infrared.

This document provides an overview of the CM SAF LST algorithm, the required input data, the physical and mathematical backgrounds of the described algorithm and it briefly describes assumptions and limitations. Details about the products' description and formats can be found

in the Product User Manual **[RD 1]**.The accuracy requirements and potential user groups are defined in the Product Requirements Document **[AD 1]**. A detailed validation of the products is shown in the Validation Report **[RD 2]**.

3 Pre-Processing

The pre-processing is performed using the GeoSatClim processing package. We require at least six valid satellite acquisitions to process data for one day. Satellite data with quality issues such as e.g. stripes or incorrect pixel values were manually deleted from the data base. A detailed description of the pre-processing algorithm implemented in GeoSatClim is available in **[RD 2]**. This section briefly summarizes relevant GeoSatClim pre-processing steps.

3.1 Meteosat radiances

3.1.1 MVIRI

MVIRI onboard MFG satellites continuously scans the full disk of the earth every 30 min. The radiometer has three spectral bands and observes the earth disk with a satellite view zenith angle (VZA) ranging from 0° to 80°. The CM SAF LST models require the MVIRI 11.5 µm thermal infrared window channel (MVIRI IR 115, Table 1, Figure 1).
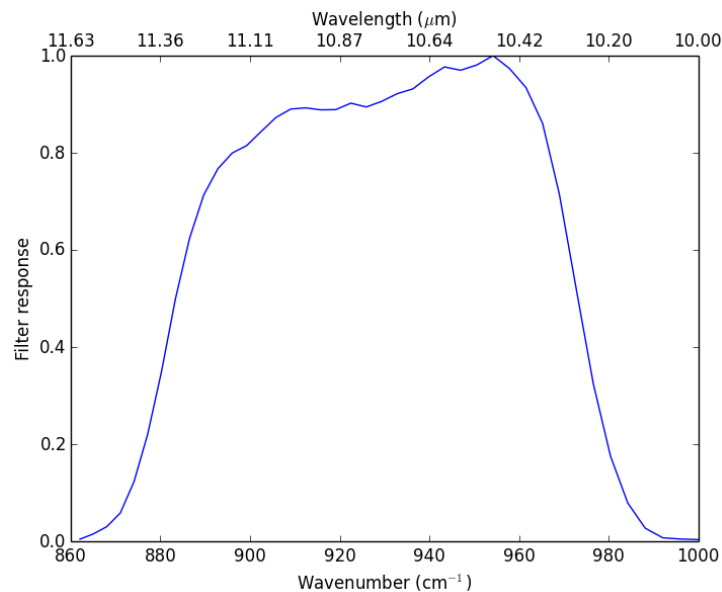
Figure 1: Spectral response of the MVIRI 11.5 µm channel.

Table 1: Properties of MVIRI's IR 115 channel.

	Nadir resolution	**Spectral range**	**Central Wavelength**
MVIRI IR 115	5 x 5 km	10.5 µm – 12.5 µm	11.5 µm

MVIRI data are available as level 1.5 files from the EUMETSAT archive. The image data is stored as digital numbers (DNs) in the OpenMTP format with slope and offset parameters. The DNs resolve approximately 0.5 K in the MVIRI IR 115 (EUMETSAT 2005).

ToA brightness temperature from MFG MVIRI are empirically related to the band integrated "effective" radiance for each infrared channel as provided by John et al. (2019):

$$T_x = \frac{\beta_x}{\ln(R_x) - \alpha_x} \tag{1}$$

where x = Water Vapour or Infraredis one of the MFG MVIRI channels and Rx is the channel band integrated "effective" radiance (mW m−2 sr−1 (cm−1)−1). The regression coefficients αx (-) and βx (K) are defined by the sensor and provided by John et al. (2019).

3.1.2 SEVIRI

SEVIRI mounted on MSG satellites provides spectral measurements in 12 channels including two thermal infrared window channels. SEVIRI samples the earth disk every 15 minutes with a spatial resolution of about 3 x 3 km^2 at nadir. The CM SAF LST algorithm uses SEVIRI's 10.8 µm data (SEVIRI IR 108). The SEVIRI IR 108 SRF is shifted about 0.7 µm to shorter wavelength compared to the corresponding MVIRI channel (Table 2, Figure 2). The sensor noise for SEVIRI's IR 108 channel is expected to be on the order of 0.15 K (www.eumetsat.int).
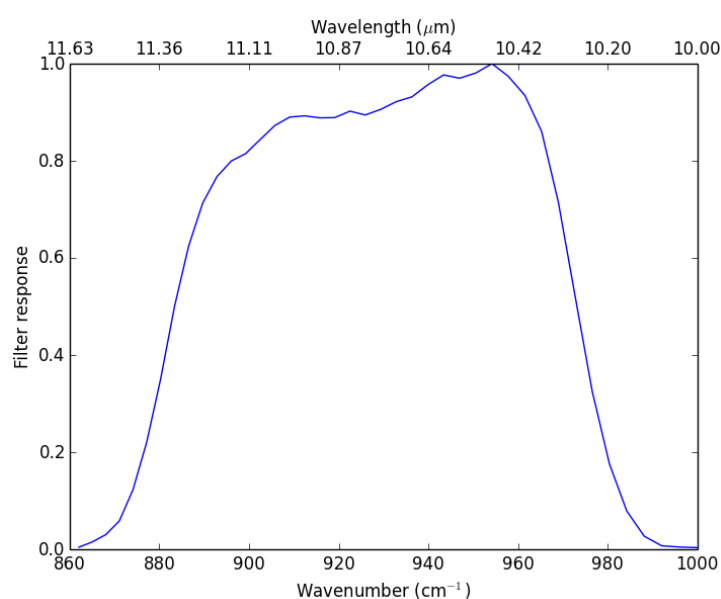
Figure 2: Spectral response of the SEVIRI 10.8 µm channel.

Table 2: Properties of SEVIRI's IR 108.

	Nadir resolution	Spectral range	Central Wavelength
SEVIRI IR 108	3 x 3 km²	9.8 μm – 11.8 μm	10.8 μm

SEVIRI level 1.5 data come as DNs in the Native format (EUMETSAT 2010), which can be converted to "effective" band-integrated radiances [mW m^{-2} sr^{-1} (cm^{-1})$^{-1}$] using equation (2). The SEVIRI IR 108 "effective" radiance can be converted to brightness temperatures by:

$$T_{ToA,10.8} = \left(\frac{c_2 \nu_{10.8}}{\ln\left(\frac{c_1 \nu_c^3}{L_{ToA,10.8}} + 1\right)} - \beta_{10.8} \right) \Big/ \alpha_{10.8} \tag{2}$$

where $c_1 = 2hc^2$ [mW m^{-2} sr^{-1} (cm^{-1})$^{-4}$], where $c_2 = \frac{hc}{\kappa}$ [K cm] and where c is the speed of light, κ is the Bolzmann constant, h is the Plancks constant and $L_{ToA,10.8}$ [mW m^{-2} sr^{-1} (cm^{-1})$^{-1}$] is the "effective" band-integrated radiances of the SEVIRI thermal channel. $\alpha_{10.8}$ [-] $\beta_{10.8}$ [K] and $\nu_{10.8}$ [cm^{-1}] are sensor specific constants which are provided by EUMETSAT for each SEVIRI instrument (EUMETSAT 2012).

3.1.3 Homogenisation

The Meteosat ToA radiance time series is not homogeneous mainly due to changing satellite instruments and instrument drifts (John et al. 2019).

For MVIRI and SEVIRI, EUMETSAT has recently initiated an inter-calibration of the MVIRI and SEVIRI IR channel against the High resolution Infrared Radiation Sounder (HIRS). HIRS, onboard NOAAs satellites, is an inter-calibrated instrument, which provides estimates of the atmospheric temperature since the late 1970s. Based on this new calibration, EUMETSAT has released updated operational correction coefficients for MVIRI and SEVIRI. The correction is available as updated slope and offset parameters on a daily basis. The inter-calibration is carried out with the SRF of the respective MVIRI and SEVIRI sensor. The exact implementation of those updated calibration parameters in GeoSatClim is described in **[RD 3]**.

The MVIRI IR 115 and the SEVIRI IR 108 channel have different SRF's (table 2 and table 3). We did not adapt the Meteosat radiance for differences in SRF. However, we took proper Meteosat SRF's in account for the radiance-based LST retrieval (see section 5) and hence indirectly correct for spectral effects.

3.2 Cloud masking

The CM SAF LST algorithm applies the CM SAF GeoSatClim two-channel cloud mask developed for MFG and MSG heritage channels **[RD 3]**. The GeoSatClim cloud mask classifies pixels as cloudy or clear on the original MVIRI or SEVIRI satellite grid. The specific logic of the cloud mask algorithm can be found in **[RD 3]** including a description of the different cloud tests.

The GeoSatClim cloud mask algorithm relies only on two Meteosat channels: the broad band visible (0.5-1.0 μm) and the thermal infrared (10-11 μm) channel available on all Meteosat instruments. Modern cloud masking algorithms, such as EUMETSAT's Nowcasting SAF (NWC SAF) cloud detection scheme, exploit the full SEVIRI spectral resolution and are hence not

applicable across Meteosat sensors. Due to missing spectral information in the short wave infrared, the cloud retrieval is under-constrained for many situations such as the cloud detection over snow and deserts **[RD 3]**. GeoSatClim replaces missing spectral information by exploiting the full temporal frequency of the Meteosat instruments **[RD 3]**. Based on 15 – 30 min clear sky ToA observations from previous acquisition days the GeoSatClim cloud retrieval algorithm models the clear sky diurnal cycle. The modelled ToA clear sky temperatures are then used as clear sky background fields for cloud masking at a specific acquisition time. Figure 4 gives an example of the diurnal temperature model implemented in the GeoSatClim cloud masking algorithm.
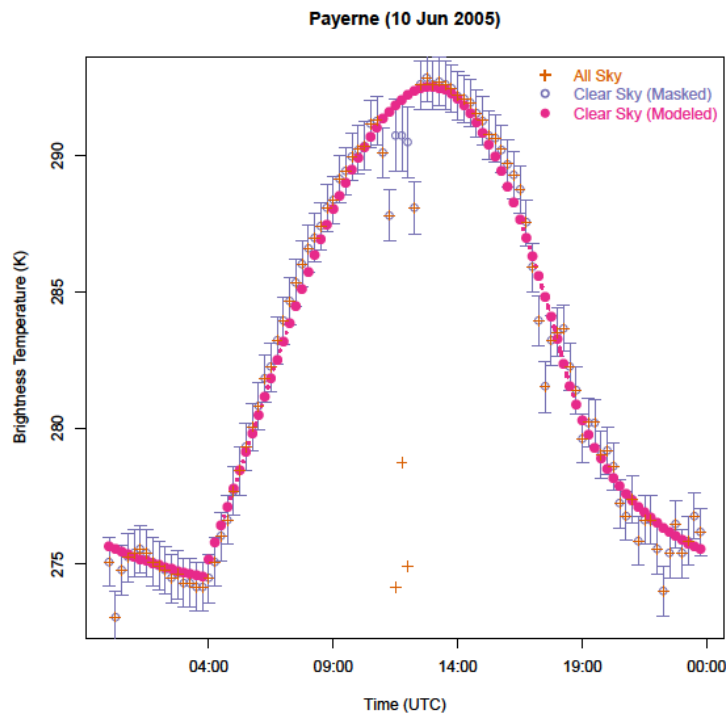
Figure 3: Example of the diurnal temperature model (Göttsche and Olesen, 2009) implemented in the GeoSatClim cloud masking algorithm. Meteosat all sky (orange crosses), cloud masked (blue circles including cloud mask uncertainty) and corresponding modeled clear sky (pink filled circles) ToA brightness temperature (image from **[RD 3]**).

4 Input data and external software

The CM SAF LST algorithm employs single-channel LST retrieval models. For single-channel LST models the LST retrieval is under-constrained and requires a-priori knowledge of the surface emissivity and the atmospheric state (Scarino et al. 2013). Moreover, radiative transfer models (RTM's) need to be used prior or during the LST processing to estimate atmospheric transmissions and emissions for a given atmospheric state. This section describes the atmospheric and surface emissivity data used as input for the CM SAF LST algorithm and it provides a brief overview about the implemented RTM model.

4.1 NWP data

Single channel LST models rely entirely on external information to estimate the atmospheric state. Atmospheric variables are taken from hourly European Center for Medium range Weather Forecasting (ECMWF) Re-Analysis (ERA 5) fields. ERA 5 data are available for the entire Meteosat time period with a ~0.3 x 0.3 latitude and longitude spatial resolution. The data are interpolated from the original ERA 5 resolution to the MVIRI/SEVIRI grid. The reanalysis data set is available on standard pressure levels. The CM SAF LST algorithm requires ECMWF temperature and specific humidity profiles at 21 pressure levels (1000 to 1 hPa) or total column water vapour fields. We interpolate the NWP data linearly between synoptic times to coincide with MVIRI / SEVIRI.

4.2 Emissivity data

We use the Combined ASTER and MODIS Emissivity over Land (CAMEL) satellite-based emissivity data (Feltz et al. 2018). This new, global high spectral resolution land surface emissivity dataset has recently been made available with a monthly and 0.05° resolution. This dataset is created by merging the Moderate Resolution Imaging Spectroradiometer (MODIS) baseline-fit emissivity database developed at the University of Wisconsin-Madison and the Advanced Spaceborne Thermal Emission and Reflection Radiometer (ASTER) Global Emissivity Dataset produced at the Jet Propulsion Laboratory. CAMEL has 13 hinge points between 3.6–14.3 m, which are expanded to cover 417 infrared spectral channels using a principal component regression approach. The CAMEL spectral emissivity is available as monthly means for the period 2000 to 2016. Based on those data we have compiled a monthly emissivity climatology.

CAMEL also provides a monthly uncertainty product. We use the CAM5K30UC v002 0.05° resolution emissivity uncertainty to estimate uncertainties for the LST retrieval (Hook 2017)

We re-project the spectral emissivities on the MVIRI / SEVIRI grid using a bilinear interpolation method. We also interpolate the monthly emissivities linearly in time to retrieve daily emissivities to avoid jumps in the final LST data set.

4.3 Radiative transfer model

Radiative transfer models (RTM's) allow the computation of the atmospheric transmissivity and the atmospheric emission for a given spectral range, if the state of the atmosphere is known. The CM SAF LST algorithm employs a RTM to compute atmospheric transmissions and emissions. The ECMWF re-analysis data, described in section 4.1, provide the atmospheric information required for the radiative transfer calculations.

The RTM implemented in the CM SAF LST algorithm is the Radiative Transfer for the TIROS Operational Vertical Sounder (RTTOV) fast radiative code (Matricardi et al. 2004). RTTOV version exists for most meteorological satellite sensor including the Meteosat MVIRI and SEVIRI sensors. For each Meteosat sensor the sensor specific RTTOV configuration files is used i.e. we account for different Meteosat instrument SRF's in the RTM runs. RTTOV offers the advantage of being very fast (Hocking et al. 2014). It is not a line-by-line RTM model, but it uses pre-computed transmittance look-up-tables (LUTs) calculated from a spectroscopic database (Hocking et al. 2014). For relatively broad satellite channels, such as e.g. the SEVIRI and MVIRI thermal window channels, reported RTTOV model errors for simulated ToA radiances are close to the satellite instrumental noise (Saunders et al. 1999). Recently Martinez et al. (2013) have shown that RTTOV can be implemented in MSG-based retrieval algorithms to produce operational satellite datasets. It calculates clear-sky atmospheric transmission, upwelling and down-welling atmospheric emissions for a given atmospheric profile and for a sensor specific spectral range.

5   Algorithm description

The CM SAF LST is derived using a single-channel approach based only on one Meteosat channel. For both MVIRI and SEVIRI we have implemented two different LST models, a Physical Mono-Window (PMW) and a Statistical Mono-Window (SMW) model. Each model produces a separate LST output.

The implemented LST models are based on single-channel models originally developed for the Geostationary Operational Environmental Satellite (GOES). The SMW model was established by the EUMETSAT LSA SAF team (Freitas et al. 2013) and was further improved and adapted to the Meteosat MVIRI and SEVIRI instruments in the framework of an EUMETSAT CM SAF – LSA SAF Federated Activity (Bento et al. 2013; Duguay-Tetzlaff et al. 2015). The presented PMW model is an adapted version of the model proposed by NASA Langley (Scarino et al. 2013) for climatological LST retrieval from single-channel infrared measurements. A detailed description of the implemented PMW and SMW model including a model inter-comparison is provided in Duguay-Tetzlaff et al. (2015).

The flow diagram for the CM SAF dual LST algorithm is presented in Figure 6.
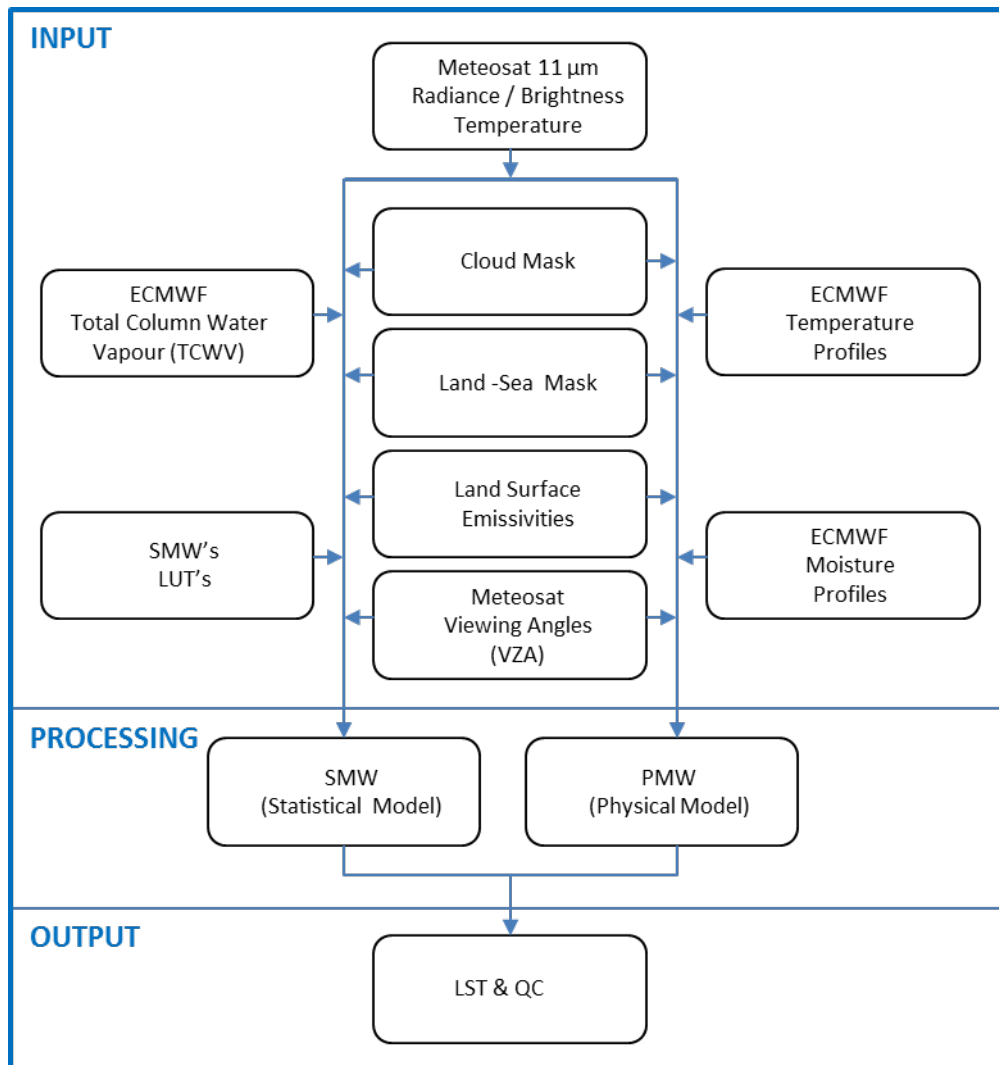
Figure 6: CM-SAF dual LST algorithm: Flow diagram for the generation of LST and respective quality control (QC).

5.1 PMW

The PMW model (Scarino et al. 2013, Heidinger et al. 2013, Duguay-Tetzlaff et al. 2015) is based on radiative transfer simulations and is described in detail in this section.

5.1.1 Background

RTM's can be used to estimate the upward and downward atmospheric path radiance ($L^{\uparrow}_{ATM,x}$, $L^{\downarrow}_{ATM,x}$) and the atmospheric transmittance ($\tau_{ATM,x}$) in the thermal infrared for a specific atmospheric profile. Approximating the Earth's surface as a Lambertian emitter-reflector and neglecting atmospheric scattering, the radiance $L_{ToA,x}$, recorded in a thermal channel onboard a satellite observing the Earth's surface can be written as (e.g. Heidinger et al. 2013):

$$L_{ToA,x} = L_{SFC,x}\,\tau_{ATM,x} + L^{\uparrow}_{ATM,x} + L^{\downarrow}_{ATM,x}(1 - \varepsilon_{SFC})\,\tau_{ATM,x} \qquad (3)$$

where x = is the sensor specific wavelength, $\varepsilon_{SFC,x}$ is the land surface emissivity at the channels wavelength and $L_{SFC,x}$ is the emission from the surface computed at the surface level.

The surface emission $L_{SFC,x}$ can be modelled as:

$$L_{SFC,x} = \varepsilon_{SFC}\,B\,(LST) \qquad (4)$$

where B () is the Planck function evaluated for the investigated thermal channel.

LST can be estimated from $L_{SFC,x}$ and $\varepsilon_{SFC,x}$ by converting the Planck Function at the sensor specific spectral range:

$$LST = B^{-1}(L_{SFC,x}/\varepsilon_{SFC,x}) \qquad (5)$$

5.1.2 PMW model description

For the MVIRI instrument the Planck function in Eq. (5) can be approximated as:

$$L_{SFC,11.5} \approx \exp\,(\alpha_{11.5} + \beta_{11.5}/LST) \qquad (6)$$

where $L_{SFC,11.5}$ is the emission from the surface [W m^{-2} sr^{-1}], $\alpha_{11.5}$ [-] and $\beta_{11.5}$ [K] are sensor specific regression coefficients provided by EUMETSAT for each MVIRI instrument (EUMETSAT 2005).

Inverting equations (6) and (3), $L_{ToA,11.5}$ [W m^{-2} sr^{-1}] measured at the sensor level can then be converted to LST:

$$\text{LST} \approx \frac{\beta_{11.5}}{\ln\left(\dfrac{L_{\text{ToA},11.5} - L_{\text{ATM},11.5}^{\uparrow} - L_{\text{ATM},11.5}^{\downarrow}\left(1 - \varepsilon_{\text{SFC},11.5}\right)\tau_{\text{ATM},11.5}}{\varepsilon_{\text{SFC},11.5}\ \tau_{\text{ATM},11.5}}\right) - \alpha_{11.5}} \qquad (7)$$

where $L_{\text{ATM},11.5}^{\uparrow}$ [W m^{-2} sr^{-1}], $L_{\text{ATM},11.5}^{\downarrow}$ [W m^{-2} sr^{-1}] and $\tau_{\text{ATM},11.5}$ [-] are the atmospheric upwelling radiance, atmospheric down-welling radiance and the atmospheric transmissivity calculated with RTTOV from ECMWF input profiles and $\varepsilon_{\text{SFC},11.5}$ [-] is the spectral MVIRI surface emissivity derived from the CAMEL Emissivity.

For SEVIRI IR108 the emission from the surface computed at the surface level ($L_{\text{SFC},10.8}$) [mW m^{-2} sr^{-1} (cm^{-1})$^{-1}$] can be approximated as:

$$L_{\text{SFC},10.8} \approx \frac{c_1 \nu_{10.8}^3}{\exp\left(\dfrac{c_2 \nu_{10.8}}{\alpha_{10.8}\,\text{LST} + \beta_{10.8}}\right) - 1} \qquad (8)$$

where $c_1 = 2hc^2$ [mW m^{-2} sr^{-1} (cm^{-1})$^{-4}$], where $c_2 = \frac{hc}{\kappa}$ [K cm] and where c is the speed of light, κ is the Bolzmann constant and h is the Plancks constant. $\alpha_{10.8}$ [-], $\beta_{10.8}$ [K] and $\nu_{10.8}$ [cm^{-1}] are sensor specific constants provided by EUMETSAT for each SEVIRI instrument (EUMETSAT 2012).

LST can then be estimated from $L_{\text{ToA},10.8}$ as:

$$\text{LST} \approx \left(\frac{c_2 \nu_{10.8}}{\ln\left(\dfrac{c_1 \nu_c^3 \tau_{\text{ATM},10.8}\,\varepsilon_{\text{SFC},10.8}}{L_{\text{ToA},10.8} - L_{\text{ATM},10.8}^{\uparrow} - L_{\text{ATM},10.8}^{\downarrow}\left(1 - \varepsilon_{\text{SFC},10.8}\right)\tau_{\text{ATM},10.8}} + 1\right)} - \beta_{10.8}\right) \Big/ \alpha_{10.8} \quad (9)$$

where $L_{\text{ATM},10.8}^{\uparrow}$ [mW m^{-2} sr^{-1} (cm^{-1})$^{-1}$], $L_{\text{ATM},10.8}^{\downarrow}$ [mW m^{-2} sr^{-1} (cm^{-1})$^{-1}$] and $\tau_{\text{ATM},10.8}$ [-] are atmospheric parameters computed with RTTOV for the SEVIRI IR 108 channel and $\varepsilon_{\text{SFC},10.8}$ [-] is the corresponding surface emissivity.

5.1.3 Preparation of PMW model terms

The PMW model follows Eq. (7) for MVIRI and Eq. (9) for SEVIRI. The model hence requires $\varepsilon_{\text{SFC},x}$, $\tau_{\text{ATM},x}$, $L_{\text{ATM},x}^{\uparrow}$ and $L_{\text{ATM},x}^{\downarrow}$ to compute LST. As stated before, these variables cannot be retrieved from a single infrared channel and hence have to be derived from an external database.

Emissivity

For the CM SAF PMW model monthly averaged emissivities from the CAMEL Emissivity Database are used. The CAMEL Database is described in section 4.2.

The emissivities are first interpolated to the exact wavelength of the MVIRI IR 115 or the SEVIRI IR 108 channel since the sampled wavelength of the emissivity files and the corresponding Meteosat instruments SRF differ (section 4.2). For each month and for each new Meteosat instrument we generate monthly emissivities by convolving the emissivities with the corresponding sensor SRF:

$$\varepsilon_{SFC,x} = \int_{x_1}^{x_2} \varepsilon_x \frac{f_x}{\int_{x_1}^{x_2} f_x} \qquad (10)$$

where $\varepsilon_{SFC,x}$ [-] is the MVIRI IR 115 or SEVIRI IR 108 spectral surface emissivity, ε_x [-] spectral resolved emissivity, f is the channel SRF and the channel wavelength x [μm] ranges from x_1 to x_2.

Atmospheric variables

We estimate the atmospheric path radiances ($L_{ATM,x}^{\uparrow}$ and $L_{ATM,x}^{\downarrow}$) and the atmospheric transmittance ($\tau_{ATM,x}$) in Eq. (7) and Eq. (9) using the RTM model RTTOV. The atmospheric temperature and moisture profiles required for RTTOV are taken from ERA5 profiles. The RTTOV RTM and the ECMWF fields are described in section 4.1.

The RTTOV simulations are performed using an adapted version of the "example fwd.F90" script available from the RTTOV source code. For each Meteosat instrument we use the specific instrument configuration file provided with the RTTOV code, which is adjusted to the instruments SRF's. We run RTTOV in a clear sky mode i.e. we do not include aerosol or cloud effects. The RTTOV simulations are performed on the original ECMWF ERA5 0.3° latitude and longitude grid at the ERA5 time steps.

The RTTOV simulations yield $L_{ATM,x}^{\uparrow}$, $L_{ATM,x}^{\downarrow}$ and $\tau_{ATM,x}$ at the ECMWF spatial and temporal resolution. The calculated atmospheric variables are hence available with a lower temporal frequency and a lower spatial resolution than the Meteosat data (4 hours versus 15-30 min, approx. 30 km versus 3-5 km) and need to be spatially and temporally interpolated to match the satellite data.
The ERA 5 grid has a lower spatial resolution compared to the satellite grid. The re-gridded atmospheric variables are hence only valid for the ECMWF grid cell height and are not necessary representative for the elevation of the Meteosat pixel. We account for those orographic effects by running RTTOV for different height levels.
First, we re-project the calculated atmospheric variables to the Meteosat grid for each height level, which yields 3 different values for $L^{\uparrow}$, $L^{\downarrow}$ and τ per Meteosat pixel. Second, we interpolate the atmospheric variables in time to match the Meteosat time steps. A third interpolation is performed for $L^{\uparrow}$, $L^{\downarrow}$ and τ calculated for different elevations to account for the exact Meteosat pixel elevation.

Please observe that RTTOV performs a simple linear extrapolation of the atmospheric temperature and water vapour profiles in case the surface height (accounted for via the surface pressure) provided is lower than the elevation of the ERA5 grid (Hocking et al. 2014). This is a very simple approximation, as the atmospheric water vapour content does not decrease

linearly with elevation. For MSG pixels with elevations above the average ERA5 pixel height, this approach follows the method proposed by Bento et al. (2017).

Figure 8 provides examples of prepared atmospheric terms for the PMW model.

30   100
Meteosat ToA 11.5 µm Radiances
$[\text{mW m}^{-2}\,\text{sr}^{-1}\,(\text{cm}^{-1})^{-1}]$

0.6   0.95
Atmospheric Transmissivity
[-]

5   35
Upwelling Atmospheric Emission
$[\text{mW m}^{-2}\,\text{sr}^{-1}\,(\text{cm}^{-1})^{-1}]$

0.95   0.99
11.5 µm Emissivity
[-]
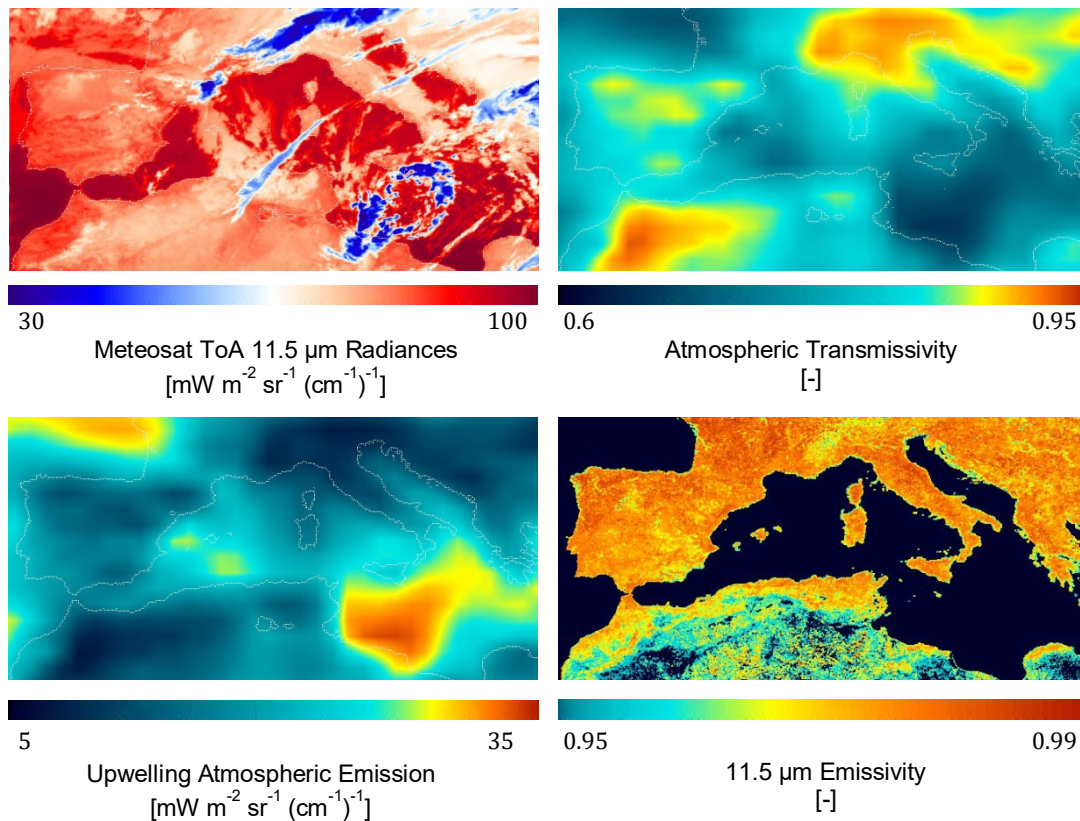
Figure 4: Examples of PMW model input. Top left: The 11.5 µm ToA radiation. Top right: The 11.5 µm atmospheric transmissivity. Bottom left: The 11.5 µm atmospheric upwelling emission. Bottom right: The 11.5 µm emissivity. Meteosat 7, January 01/01/2005 00:00 am.

5.2 SMW

SMWs consist of empirical approaches that relate ToA brightness temperatures of a single infrared window channel directly to LST. The infrared radiative transfer is generally approximated via a simple linear regression. The CM SAF SMW model (Bento et al. 2013, Duguay-Tetzlaff et al. 2015) uses a formulation close to that proposed within the context of Copernicus Global Land Service (CGLS) (Freitas et al. 2013).

5.2.1 SMW model description

The CM SAF SMW (Bento et al. 2013, Duguay-Tetzlaff et al. 2015) linearizes the radiative transfer equation Eq.(3), while at the same time maintaining an explicit dependency on the surface emissivity. Thus, LST [K] is a function of the MVIRI IR 115 or the SEVIRI IR 108 clear sky ToA brightness temperature ($T_{\text{ToA,X}}$) [K]:

$$LST = A \, \frac{T_{ToA,X}}{\varepsilon_{SFC,x}} + B \, \frac{1}{\varepsilon_{SFC,x}} + C \qquad\qquad \textbf{(11)}$$

where $\varepsilon_{SFC,x}$ [-] is the spectral surface emissivity calculated using the CAMEL emissivity (see section 4.2). A [-], B [-] and C [-] are the SMW calibration coefficients obtained by fitting Eq. (11) to the calibration database described in the following section.

5.2.2 SMW model calibration

The SMW model calibration relies on radiative transfer simulations of $T_{ToA,X}$ for the MVIRI IR 115 or the SEVIRI IR 108 channel for a database of global temperature and moisture profiles referred to as SeeBor (Borbas et al. 2005). We strictly followed the method applied by the LSA SAF team to tune its operational dual-channel **[RD 4]** and the GOES single-channel LST model (Freitas et al. 2013).

The SeeBor database (Borbas et al. 2005) includes over 15,000 atmospheric profiles representative for global conditions. Each profiles is associated with a spectrally resolved land surface emissivity and a LST estimated from T_{2m} observations. The LSA SAF team has carefully selected 116 profiles within the Meteosat disk to tune the presented single-channel SMW model in Eq. (11). The profiles cover a wide range of atmospheric conditions ranging from very dry to very moist atmospheres.

The RTM simulations are performed with the line-by-line MODerate resolution atmospheric TRANsmission model MODTRAN (Berk et al. 1999). A total of over 845,000 $T_{ToA,X}$ simulations were obtained by varying the viewing geometry and surface conditions for each selected profile over the following ranges: (1) VZA from 0° to 75°; (2) surface emissivity between 0.926 and 0.998 and (3) LST ranging from near surface air temperature minus 15 K to near surface air temperature plus 15 K. For each Meteosat instrument separate simulations are performed to account for different Meteosat SRF's.

The regression coefficients A, B, and C in Eq. (11) were estimated for each Meteosat instrument separately using the simulated $T_{ToA,X}$ and the corresponding LST's. The coefficients were determined for 8 different TCWV classes (0 cm to 6 cm in steps of 0.75 cm) and 15 VZA classes (0° to 75° in steps of 5°). This yields 7 LUTs for the MVIRI instrument (Meteosat 1 to 7) and 3 LUTs for MVIRI (MSG 1 to 3) including A, B and C estimates for each TCWV / VZA classes. The model hence accounts for different atmospheric conditions (TCWV) and differences in atmospheric path length (VZA).

5.2.3 Preparation of SMW model terms

The SMW model presented in Eq. (11) requires information about the spectral surface emissivity ($\varepsilon_{SFC,x}$). In addition, information about atmospheric TCWV's and satellite VZA's are necessary to selected the proper class from the SMW LUTs (examples Figure 9).

The VZA's are calculated in GeoSatClim **[RD 3]** for each satellite pixel separately. They are handled as dynamic fields and are re-adjusted for every Meteosat instrument and every time the satellite changes position **[RD 3]**.

The $\varepsilon_{SFC,x}$ is computed similar to the PMW $\varepsilon_{SFC,x}$ model term using the adapted spectral emissivities from the CAMEL Emissivity Database (see section 4.2 and 5.1.3).
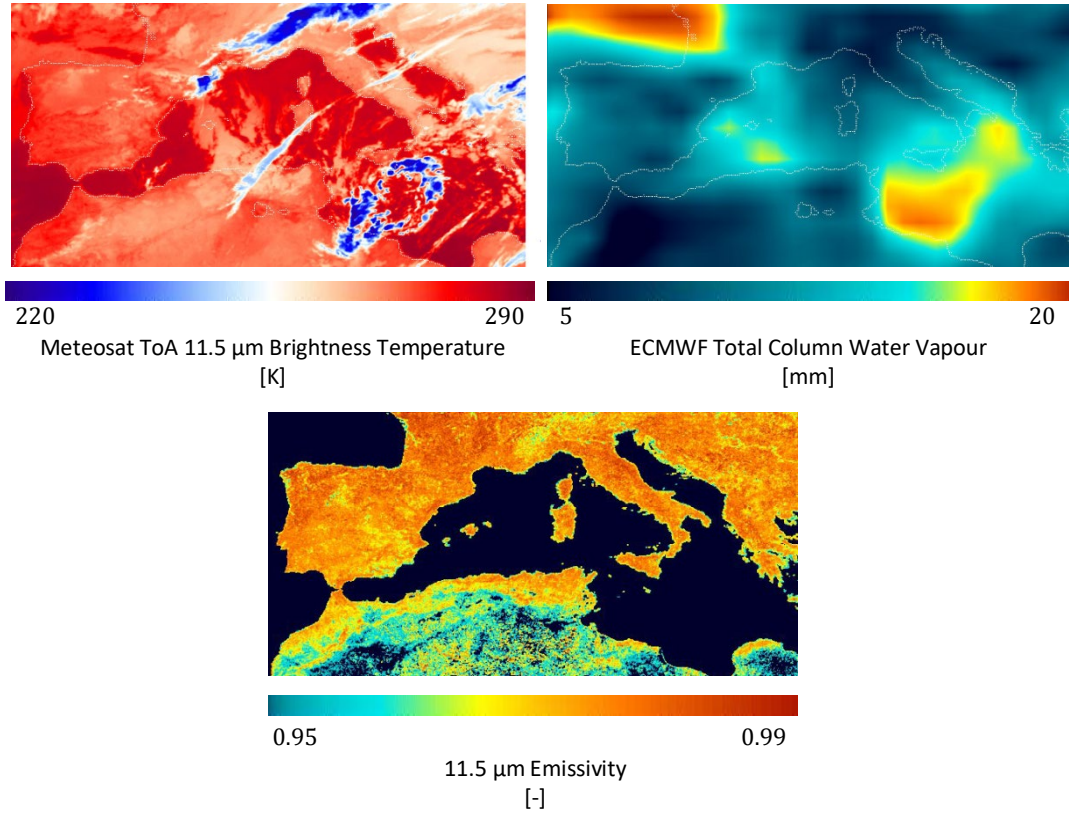

Figure 5: Examples of SMW model input. Top left: The ToA 11.5 μm brightness temperature. Top right: ERA5 total column water vapour. Bottom: The 11.5 μm emissivity. Meteosat 7, January 01/01/2005 00:00 am.

The SMW model makes use of ERA5 TCWV fields (see section 4.1). The ERA TCWV pixels are re-projected to the Meteosat satellite grid. The ERA5 grid has a significantly lower spatial resolution compared to the satellite grid. The re-gridded TCWV values are hence only valid for the ECMWF grid cell height (Z_{ECMWF}, [m]) and are not necessary representative for the Meteosat pixel height ($Z_{Meteosat}$, [m]). We account for those orographic effects by adapting the ECMWF TCWV ($TCWV_{ECMWF}$, [cm]) through an exponential relationship to the Meteosat TCWV ($TCWV_{Meteosat}$, [cm]) (Bento et al. 2017):

$$TCWV_{Meteosat} = TCWV_{ECMWF} * \exp(\frac{Z_{ECMWF} - Z_{Meteosat}}{\alpha_{Height}}) \tag{12}$$

where $\alpha_{Height} = 1581.4$ [m]. α_{Height} is obtained by fitting equation (12) to a training data base.

6   Uncertainty characterisation

The CM SAF LST uncertainty characterisation follows the LSA SAF LST algorithm **[RD 4]** to achieve a maximum consistency between the two algorithms.

Potential LST uncertainties were assessed through the use of a synthetic validation database. The validation data base is constructed from radiative transfer simulations of ToA MVIRI IR 115 and SEVIRI IR 108 radiance for SeeBor atmospheric profiles (Borbas et al. 2005), which are not used for the SMW model calibration (see section 5.1.2). We provided ToA brightness temperatures, surface and atmospheric information from the database as input to the SMW and PMW model; the calculated LST output was then compared with the corresponding ("true") surface temperature from the database.

The LST uncertainty, S_{LST}, is composed of three components: 1) radiometric noise, 2) uncertainty in surface emissivity and 3) uncertainty in NWP profiles. All error sources are considered to be independent:

$$S_{LST} = \sqrt{S_{noise}^2 + S_{emissivity}^2 + S_{NWP}^2} \tag{13}$$

1) Radiometric noise
The value used for SEVIR radiometric noise is based on radiometric performances defined as short term errors that include random noise, temperature of detectors, crosstalk and straylight stability of gain and electromagnetic perturbation. The values for noise in ToA radiances were generated from a uniform random distribution within the conservative interval [-0.3 K, 0.3 K] for SEVIRI (Schmetz et al. 2002). The MVIRI noise [-1.3 K, 1.3 K] corresponds to the mean absolute bias reported in **[RD 3]** for a comparison of SEVIRI 108 and MVIRI 115 ToA radiances for the Swiss station Payerne in 2005.

2) Uncertainty in surface emissivity
The uncertainty in surface emissivity is estimated using the CAMEL monthly uncertainty product (see also chapter 4.2).

3) Uncertainty in NWP profiles
The PMW model requires a characterization of the uncertainties associated with the atmospheric profiles. Since these are obtained from ERA5 nearest in space and time to the satellite observation, we assume that the uncertainty in collocation may be used as a measure of the profile uncertainty. Thus, the impact of profile errors on retrieved LST values was estimated by replacing the profiles at hour h by the corresponding ones at hour h+6. A similar procedure was used to determine the impact of TCWV errors on LST estimates from the SMW.

7 Spatial and temporal aggregation

The two algorithms described in the previous sections allow the estimation of LST on a pixel-by-pixel basis. The calculated LST corresponds to instantaneous fields produced every 15 minutes in the case of SEVIRI and 30 minutes in the case of MVIRI.

The individual LST fields are re-projected and merged onto a 0.05° x 0.05° regular latitude and longitude grid, covering the geographic range of 65° N to 65° S and 65° W to 65° E. Re-projected, instantaneous fields are aggregated into hourly, daily and monthly means. For each aggregation, the number of actual LST retrievals are provided as ancillary data in the output files. The spatial and temporal aggregation is conducted using the GeoSatClim re-projection and aggregation tools **[RD 3]**.

7.1 Hourly aggregation

We provide hourly samples and do not calculate hourly means. LST has a strong diurnal cycle and hourly means can be biased in case observations are missing. As example:

- MFG and MSG: the 12 hourly sample is composed of the full disk scan starting at 12:00 UTC.

7.2 Monthly aggregation

The monthly LST compositing is performed for the daily cycle. The monthly mean diurnal LST cycle is estimated as the arithmetic mean of hourly sample data on a pixel basis over the different days of the month. Hence, it consist of 24 values containing the hourly means for the respective month. We require at least 3 hourly samples to be present per month and time step to calculate the monthly diurnal cycle composites.

8   Assumptions and limitations

The retrieved LST value is an effective LST over isothermal mixed pixel. The major constrain of the presented algorithm is its restriction to clear sky observations as it uses thermal infrared satellite bands. It is hence only applicable on cloudless pixels. In addition, the implemented CM SAF LST algorithm presents the following limitations:

1) Dependency on NWP

The ability to estimate LST from a single infrared channel is highly dependent on the correct estimation of the atmospheric absorption (Freitas et al. 2010). In contrast to the Generalized Split-Window Model **[RD 4]**, which is used to generate the LSA SAF MSG LST product, the atmospheric absorption cannot be estimated through a two-channel regression of satellite ToA brightness temperatures. Hence, single-channel LST models depend entirely on ancillary data from Numerical Weather Prediction (NWP) models to estimate the atmospheric state. This dependency on NWP is the price for a consistent LST retrieval scheme applicable across all Meteosat satellite generations.

2) Emissivity assumptions

LST effects due to directional emissivity features and emissivity variation in a pixel are not considered in the presented algorithm. Moreover, the presented LST algorithm uses a constant, monthly emissivity for all Meteosat acquisitions. Emissivity variations due to land cover changes are thus not accounted for, despite their relevance for the LST retrieval. LST inaccuracies can be up to 3 K for wrongly assigned surface emissivities in arid regions (Freitas et al. 2010). We also interpolate the emissivities linearly in space and time, which does not necessary reflect the true spatial and temporal variations as we are dealing with non-linear properties.

3) Dependency on TCWV

Single-channel LST models are likely to be inaccurate in regions with heavy atmospheric water vapour loading (Freitas et al. 2013, Heidinger et al. 2013, Duguay-Tetzlaff et al. 2015). For an optical dense atmosphere (TCWV > 50 mm), slightly inaccurate atmospheric input fields can lead to LST retrieval uncertainties up to 6 K for SMWs (Freitas et al. 2013) and up to 10 K for PMWs (Duguay-Tetzlaff et al. 2015). For the presented Meteosat-based LST, we expect less than 5 % of all retrievals to be associated with those high TCWV's since very humid atmospheres primarily occur in tropical and subtropical regions, which are regularly cloud covered (Duguay-Tetzlaff et al. 2015).

4) Dependency on VZA

Geostationary satellite-based LST retrievals dependent on the satellite viewing geometry and can vary up to 6 K or more with increasing VZA (Scarino et al. 2013). VZA effects due to roughness and structure of land surface are not handled in the presented algorithm. Shaded surfaces are e.g. significantly cooler than sunlit surfaces and the apparent shadow fraction in a pixel varies with the satellite viewing and sun geometry. The presented single-channel models account for differences in atmospheric path length due to different VZA's. However, Freitas et al. (2013) have demonstrated that single-channel models are unstable for high VZA's (> 65°) and moderate to moist atmospheres (TCWV > 30 mm). This is due to the increasing atmospheric path length with increasing VZA's. We therefore limit the LST retrieval to a Meteosat view zenith angle (VZA) below 70°. This definition follows the VZA restrictions implemented for the operational LSA SAF LST algorithm **[RD 4]**. Within the MSG disk the atmosphere is often fairly dry for large VZA's partially compensating for the poorer model performance due to the long optical path **[RD 4]**.

9   Directions for future improvements

Directions for future improvement of the CM SAF LST algorithm include:

1) Enhanced emissivity data

Clearly, accurate land surface emissivity input is very important to its retrieved LST. It is planned to use dynamic emissivity maps instead of monthly averages. Vegetation re-analysis data, such as the 50 year long daily global phenology data set created by Stöckli et al. (2011), might be used to account for temporal changes in vegetation cover. Those data could be combined with the currently implemented emissivities to create monthly emissivity maps for all Meteosat years.

2) Reduced VZA dependencies

Scarino et al. (2013) have demonstrated that it is possible to reduce uncertainties in geostationary LST retrievals due to VZA dependencies by about 10%. They propose an empirical model which relates MODIS nadir views and off nadir views from geostationary satellite data (here GOES) for different seasons and acquisition times. Such an empirical model could be established for Meteosat.

3) Improved daily averaging

We have implemented a very simple method to produce daily LST's by calculating the arithmetic mean from available hourly LST data. As LST's vary strongly in time (Göttsche et al. 2009) this approach is highly inaccurate for hourly averages spread unequally over daylight times. To overcome this problem, we propose to fit a thermal model, such as e.g. the model by Mannstein et al. (1999) or by Göttsche and Olesen (2009), to the observed LST's to re-construct the entire diurnal LST cycle. The daily LST product might then be calculated from observed and modelled LST.

4) Improved uncertainty estimation

The CM SAF LST uncertainty characterization does not distinguish between random and systematic noise. Moreover, it assumes a constant sensor noise for both MVIRI and SEVIRI. Within the upcoming years EUMETSAT will issue updated operational correction coefficients for all Meteosat infrared sensors associated with uncertainty information (V. John, R. Roebling and J. Schulz, personal communication). In addition, the Horizon 2020 project FIDUCEO is developing new methods to characterize all significant uncertainty components of satellite-based TCDR's by introducing concepts from metrology such as traceability and error propagation. It should be exploited if this new techniques can be implemented in the CM SAF LST algorithm.

5) Quasi-global LST

The CM SAF LST algorithm could be extended to other geostationary and polar orbiting sensors. Most geostationary and polar orbiting imagers have a thermal window channel centered around 11 µm. The existing algorithm can hence be easily adapted to most modern satellite imagers. It would need to be tested weather LST uncertainties due to different satellite viewing geometries are sufficiently small to create a consistent, global LST TCDR from combined polar orbiting and geostationary imagers. Moreover, the feasibility to produce all sky LST data from combined microwave and infrared measurements could be evaluated.

10 References

Bento, V., Exploring RTTOV to retrieve Land Surface Temperature from a geostationary satellite constellation, Master thesis, University of Lisboa, Portugal, 2013.

Berk, A., G. Anderson, P. Acharya, J. Ghetwynd, L. Bernstein, E. Shettle, M. Matthew and S. Adler-Golden, MODTRAN4 User's Manual, Air Force Research Laboratory, USA, 1999.

Bento, V.A., C.C. DaCamara, I.F.Trigo, J.P.A. Martins and A. Duguay-Tetzlaff, Improving Land Surface Temperature Retrievals over Mountainous Regions. Remote Sens., 2017.

Borbas, E.E., S.S. Wetzel, H. L. Huang and J. Li, Global profile training database for satellite regression retrievals with estimates of skin temperature and emissivity, Proc. of the of the XIV International ATOVS Study Conference, Beijing, China, 25-31 May 2005.

Dee, D. P., S. M. Uppala, A. J. Simmons, P. Berrisford, P. Poli, S. Kobayashi, U. Andrae, M. A. Balmaseda, G. Balsamo, P. Bauer, P. Bechtold, A. C. M. Beljaars, L. van de Berg, J. Bidlot, N. Bormann, C. Delsol, R. Dragani, M. Fuentes, A. J. Geer, L. Haimberger, S. B. Healy, H. Hersbach, E. V. Holm, L. Isaksen, P. Kallberg, M. Kohler, M. Matricardi, A. P. McNally, B. M. Monge-Sanz, J.-J. Morcrette, B.-K. Park, C. Peubey, P.de Rosnay, C. Tavolato, J.-N. Thepaut and F. Vitart, The era-interim reanalysis: configuration and performance of the data assimilation system, Q. J. R. Meteorol. Soc., 137, 2011.

Duguay-Tetzlaff, A., V. A. Bento, F. M. Göttsche, R. Stöckli, J. P. A. Martins, I. Trigo, F. Olesen, J. S. Bojanowski, C. da Camara and H. Kunz, Meteosat land surface temperature climate data record: Achievable accuracy and potential uncertainties, Remote Sens., 2015.

Feltz, M., E. Borbas, R. Knuteson, G. Hulley and S. Hook,The Combined ASTER MODIS Emissivity over Land (CAMEL) Part 2: Uncertainty and validation. Remote Sens., 2018.

EUMETSAT, Operational service meteosat-7 calibration report issue 30. Technical Report EUM/OPS/REP/05/1938, EUMETSAT, Am Kavalleriesand 31, D-64295 Darmstadt, Germany, 2005.

EUMETSAT, Meteosat vis channel calibration information, EUMETSAT, Am Kavalleriesand 31, D-64295 Darmstadt, Germany, 2010.

EUMETSAT, The conversion from effective radiances to equivalent brightness temperatures, Technical Report EUM/MET/TEN/11/0569, EUMETSAT, D-64295 Darmstadt, Germany, 2012.

Freitas, S., I. Trigo, J. Bioucas-Dias and F. Göttsche, Quantifying the uncertainty of land surface temperature retrievals from SEVIRI/METEOSAT, IEEE Transactions on Geoscience and Remote Sensing, 48, 2010.

Freitas, S., I. Trigo, J. Macedo, C. Barroso, R. Silva, and R. Perdigao, Land surface temperature from multiple geostationary satellites, International Journal of Remote Sensing, 34, 2013.

Göttsche, F. and F. Olesen, Modelling the effect of optical thickness on diurnal cycles of land surface temperature, Remote Sensing of Environment, 113, 2009.

Heidinger, A., I. Laszlo, C. Molling and D. Tarpley, Using Surfrad to verify the NOAA single-channel land surface temperature algorithm, Journal of Atmospheric and Oceanic Technology, 30, 2013.

Hook, S.. Combined ASTER and MODIS Emissivity database over Land (CAMEL) Uncertainty Monthly Global 0.05Deg V002. 2017, distributed by NASA EOSDIS Land Processes DAAC, https://doi.org/10.5067/MEaSUREs/LSTE/CAM5K30UC.002. Accessed 2020-09-14.

Hocking, J., P.J. Rayer, D. Rundle, R.W. Saunders, M. Matricardi, A. Geer, P. Brunel and J. Vidot, RTTOV v11 Users Guide, Nowcasting Satellite Application Facility (NWC-SAF), 2014.

John, V. O., Tabata, T., R¨uthrich, F., Roebeling, R., Hewison, T., St´´ockli, R., and Schulz, J., On the methods for recalibrating geostationary longwave channels using polar orbiting infrared sounders. Remote Sensing, 2019.

Matricardi, M., F. Chevallier, G. Kelly and J. N. Thépaut, An improved general fast radiative transfer model for the assimilation of radiance observations, Quat. J. Roy. Meteor. Soc., 130, 2004.

Karl, T. R. , P. D. Jones, R. W. Knight, G. Kukla, N. Plummer, V. Razuvayev, K. P. Gallo, J. Lindseay, R. J. Charlson and T. C. Peterson, A new perspective on recent global warming, Bull. Am. Meteorol. Soc. 74, 1993.

Hewison, T. J., and M. König, Inter-calibration of Meteosat imagers and IASI, Proc. of the EUMETSAT Meteorological Satellite Conference, Darmstadt, Germany, 8-12 September 2008.

Mannstein, H., Broesamle, H., Schillings, C., and F. Trieb, Using a Meteosat cloud index to model the performance of solar thermal power stations, Proc. of the EUMETSAT Meteorological Satellite Data Users' Conference, Copenhagen, Denmark, 6-10 September 1999.

Martinez, M. A., M. Manso and P. Fernández, Algorithm Theoretical Basis Document for "SEVIRI Physical Retrieval Dataset" (SPhR-PGE13 v2.0), Nowcasting Satellite Application Facility (NWC-SAF), 2013.

Saunders, R., M. Matricardi and P. Brunel, An improved fast radiative transfer model for assimilation of satellite radiance observations, Quarterly Journal of the Royal Meteorological Society, 125, 1999.

Scarino, B., P. Minnis, R. Palikonda, R. Reichle, D. Morstad, C. Yost, B. Shan and Q. Liu, Retrieving clear-sky surface skin temperature for numerical weather prediction applications from geostationary satellite data, Remote Sensing, 5, 2013.

Schmetz, J., P. Pili, S. Tjemkes, D. Just, J. Kerkann, S. Rota and A. Ratier, An introduction to Meteosat Second Generation (MSG), Bulletin of the American Meteorological Society 83, 2002.

Seemann, S.W., E. E. Borbas, R. O. Knuteson, G. R. Stephenson and H. L. Huang, Development of a Global Infrared Land Surface Emissivity Database for Application to Clear Sky Sounding Retrievals from Multi-spectral Satellite Radiance Measurements, J. of Appl. Meteor. and Climatol., 47, 2008.

Stöckli, R., T. Rutishauser, I. Baker, M. Liniger and A. S. Denning, A global reanalysis of vegetation phenology, J. Geophys. Res. - Biogeosciences, 116, 2011.

Sun, D. L., R. T. Pinker and M. Kafatos, Diurnal temperature range over the United States: A satellite view, Geophys. Res. Lett., 33, 2006.

11 Glossary

ATBD	Algorithm Theoretical Basis Document
AVHRR	Advanced Very High Resolution Radiometer
CDOP	Continuous Development and Operations Phase
CM SAF	Climate Monitoring Satellite Application Facility
DN	Digital Number
DWD	Deutscher WetterDienst
ECMWF	European Center for Medium-range Weather Forecast
ECV	Essential Climate Variables
ERA5	ECMWF ReAnalysis
EUMETSAT	EUropean organisation for the exploitation of METeorological SATellites
FCDR	Fundamental Climate Data Record
FMI	Finnish Meteorological Institute
GCOS	Global Climate Observing System
GOES	Geostationary Operational Environmental Satellite
HIRS	High resolution Infrared Radiation Sounder
KNMI	Royal Meteorological Institute of the Netherlands
LSA SAF	Land Surface Analysis Satellite Applications Facility
LST	Land Surface Temperature
LUT	Look-Up-Table
MeteoSwiss	Meteorological Service of Switzerland
MFG	Meteosat First Generation
MODIS	MODerate resolution Imaging Spectrometer
MODTRAN	MODerate resolution atmospheric TRANsmission model
MSG	Meteosat Second Generation
MVIRI	Meteosat Visible and InfraRed Imager
NASA	National Aeronautics and Space Administration (USA)
NOAA	National Oceanic and Atmospheric Agency
NWP	Numerical Weather Prediction
PMW	Physical Mono-Window
QC	Quality Control
RMIB	Royal Meteorological Institute of Belgium
RTM	Radiative Transfer Model
RTTOV	TIROS Operational Vertical Sounder radiative code
SAF	Satellite Application Facility
SEVIRI	Spinning Enhanced Visible and InfraRed Imager
SMHI	Swedish Meteorological and Hydrological Institute
SMW	Statistical Mono-Window
SRF	Spectral Response Function
ToA	Top of Atmosphere
TCDR	Thematic Climate Data Record
TCWV	Total Column Water Vapour
UK MetOffice	Meteorological Service of the United Kingdom
VZA	Satellite view Zenith Angle